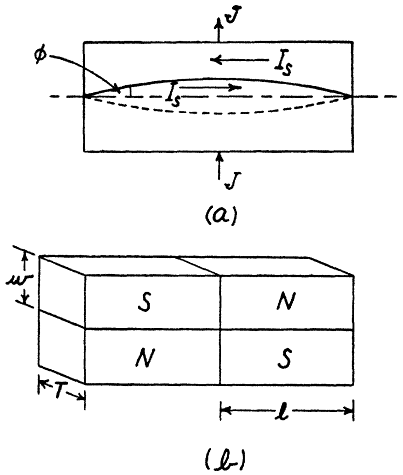

FIG. 1. (a) Top view of one leg of rectangle. (b) Approximate pole distribution due to gradual bending of wall.

using the boundary condition $x'=0$ when $y=\pm T/2$. The result is

$$\tfrac{1}{2}a[\tfrac{1}{4}T^2-y^2]=(K_2x'/2K_1)+2x'\ln(2/x'),$$

where

$$a=4\phi JI_s/10TL(K_1A)^{\frac{1}{2}}.$$

The form of the result is convenient for estimating the effect of the K_2 term.

It did not prove to be feasible to integrate again analytically. A numerical integration was carried out to determine the wall displacement, W. In this work the crystal dimensions given in reference 1 were used. The results given in Table I were obtained, taking $K_1=4.2\times10^5$ ergs/cm^3, and $K_2=1.5\times10^5$ ergs/cm^3 for iron. Here, J_I is the current without the K_2 correction, while J_{II} includes the K_2 term. The shape of the wall is effectively unchanged by the K_2 correction. Each value of W corresponds to a value of λ_{max}. The validity of the assumption of small λ is doubtful for $\lambda_{max}=0.3$. For the representative value $\lambda_{max}=0.1$, the K_2 correction is only about 2 or 3 percent.

In the preceding work the assumption was made that, although the current is applied at only one cross section of the crystal, the deformation caused in the wall is the same all around the crystal. This assumption is now justified by showing that a wall only locally deformed would give rise to a magnetostatic contribution to the crystal energy much larger than the excess energy of the wall due to its deformation. Looking at the leg to which the current is applied from the top, and assuming the wall to bend gradually back to its normal position, we see the situation shown in Fig. 1(a).

The discontinuity in the normal component of the saturation magnetization as a result of the curving wall results in a pole distribution which can be approximated by the arrangement of Fig. 1(b), where the pole density in each region is approximately $I\sim I_s\bar{\lambda}T/l$. Here, $\bar{\lambda}$ is the average angle the wall makes with the y axis. Considering the right-hand half only, the magnetostatic energy density can be approximated by the expression for the surface energy density of a series of coplanar strips, $\sigma_{ms}=0.85I^2w$. Hence, the total magnetostatic energy is

$$W_{ms}\sim(I_s\lambda T/l)^2w\cdot w\cdot l.$$

The deformation wall energy is $\delta W_{wall}\sim\sigma_w lT\lambda^2$. Therefore, using as rough estimates $T\sim w\sim0.1$ cm, $\sigma_w\sim1$ erg/cm^2, $l\sim1$ cm, we obtain $\delta W_{wall}/W_{ms}\approx10^{-3}$. Hence, the wall can be assumed to be uniformly deformed around the crystal circumference to within about 3 percent.

I wish to thank Professor Charles Kittel for suggesting this work and for many helpful discussions.

[1] H. J. Williams and W. Shockley, Phys. Rev. 75, 178 (1949).
[2] Williams, Shockley, and Kittel, to be published.
[3] L. Néel, Cahiers phys. 25, 1 (1944).

The Spin of Be^9

N. A. SCHUSTER AND G. E. PAKE*
Physics Department, Washington University, St. Louis, Missouri
January 4, 1951

DIRECT experimental evidence that the spin of Be^9 is 3/2 has been obtained from studies of the Be^9 nuclear magnetic resonance in a single crystal of $BeAl_2O_4$ (chrysoberyl). Previous information concerning the spin of Be^9 was obtained by Paul[1] from hyperfine structure studies of the BeII resonance line $\lambda=3130$A. Paul's work ruled out spin 5/2, and, although spin 3/2 seemed most probable, spin 1/2 remained a possibility.

Be^9 resonances, two of which are shown in Fig. 1, were obtained with a recording r-f spectrometer at a number of orientations of the $BeAl_2O_4$ crystal in the magnetic field of about 7300 gauss. Each resonance has three components clearly discernible, the large central component falling near 4.377 Mc/sec. The displacement of the satellites from the central line varies, depending upon crystal orientation in the magnetic field, from essentially zero to 240 kc/sec for the crystal orientations thus far investigated.

Since the electric quadrupole interaction of a nucleus of spin $I>1/2$ with the gradient of an electric field breaks the nuclear resonance into $2I$ components,[2] the observed resonances offer reasonably unambiguous evidence for spin 3/2 if a quadrupole interaction is responsible for their structure.

Although it might be suggested that the splitting could originate with nuclear magnetic dipole-dipole interactions, which are known to produce resolvable splittings of resonances in certain crystals,[3] the observed Be^9 splitting exceeds by nearly two orders

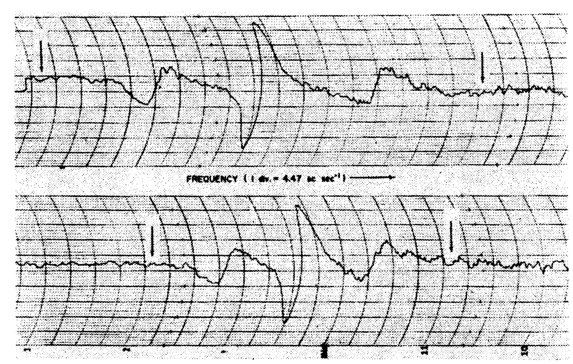

FIG. 1. Absorption curve derivatives of Be^9 magnetic resonances in a single crystal of $BeAl_2O_4$ for two crystal orientations in the magnetic field. The three quadrupole components of each resonance verify that the spin of Be^9 is 3/2. Vertical arrows mark the approximate positions at which additional components should occur if the patterns are quadrupole splittings corresponding to spin 5/2.

of magnitude that which could arise from the strongest nuclear dipole-dipole interaction in the chrysoberyl lattice. The lattice is orthorhombic[4] without simple axial symmetry and detailed information concerning the electric field gradient is not available. Therefore, quantitative studies of the variation of splitting with crystal orientation can neither establish the quadrupole interaction nor measure the electric quadrupole moment of Be^9. However, qualitative features of the variation with orientation, relative intensities of the component lines, and the magnitude of the splitting are consistent with known quadrupole splittings observed by Pound[2] and observed in this laboratory.[5]

If the observed lines were the three central lines of a five-component pattern corresponding to spin 5/2, additional weaker satellites should appear near the positions marked by the arrows in Fig. 1. Failure to observe such additional satellites in any of the experimental resonances confirms Paul's conclusion that the spin of Be^9 is not 5/2. The mere existence of an electric quadrupole moment eliminates spin 1/2, and it seems safe to conclude that the spin of Be^9 is definitely 3/2.

We wish to thank W. G. Zinn and R. H. Sands for assistance in taking the data.

* Assisted by the joint program of the ONR and AEC.

[1] W. Paul, Z. Physik **117**, 774 (1941).
[2] R. V. Pound, Phys. Rev. **79**, 685 (1950).
[3] G. E. Pake, J. Chem. Phys. **16**, 327 (1948).
[4] W. L. Bragg and G. B. Brown, Z. Krist. **63**, 122 (1926).
[5] N. A. Schuster and G. E. Pake, Phys. Rev. **81**, 157 (1951).

Magnetic Domain Patterns on Nickel Crystals

MIKIO YAMAMOTO AND TAKAO IWATA
Research Institute for Iron, Steel, and other Metals, Tôhoku University, Sendai, Japan
December 18, 1950

WE have succeeded in observing the magnetic powder patterns on single crystals of pure nickel whose ferromagnetic anisotropy constant $K<0$. These patterns are as simple and interpretable as those obtained by Williams and his collaborators on crystals of an iron-silicon alloy containing 4 percent silicon[1] ($K>0$) and of a nickel-cobalt alloy containing 60 percent cobalt[2] ($K<0$). The surfaces of our crystals were polished parallel to the $(\bar{1}10)$ planes very carefully, and were annealed in vacuum and polished electrolytically. The powder patterns formed with magnetite colloid were observed under the microscope with the usual light field with vertical illumination.

Two of the typical patterns and their interpretations are shown in Figs. 1 and 2. In Fig. 1 the 180° and 109° walls form the parallelogram net, and short 71° walls are also in evidence at the corners of the parallelograms. This pattern is similar to that observed on a cobalt-nickel crystal by Walker and Bozorth.[2] In addition, the tree pattern of which the trunk is the 180° wall, corresponding to the tree pattern of the first kind on the (100) planes of silicon-iron crystals,[1] is seen. In this tree pattern the angles between the branches and the trunk are about 35° and 55° on both sides of the trunk, as is expected theoretically. Moreover, as the inclination of the surface to the $(\bar{1}10)$ plane becomes larger, the branches do not become thicker but radiate smaller secondary, ternary, and other branches.

Figure 2 shows the 71° walls and the tree pattern of the second kind of which the trunk is the 71° wall. The surface of the crystal coincides with the $(\bar{1}10)$ plane at the middle of the upper part of the figure, and on the lower and left-hand parts it is inclined to the crystal plane. When this inclination is slight, the 71° wall becomes the trunk and radiates branches perpendicularly on both sides. As the inclination increases, however, branches of another type, making an angle of about 35° with the trunk, are radiated symmetrically; and thus the magnetostatic energy is greatly reduced. It is to be added that there have been observed also branches perpendicular to the trunk of the 109° wall, belonging to a third kind of tree pattern which is to be expected theoretically.

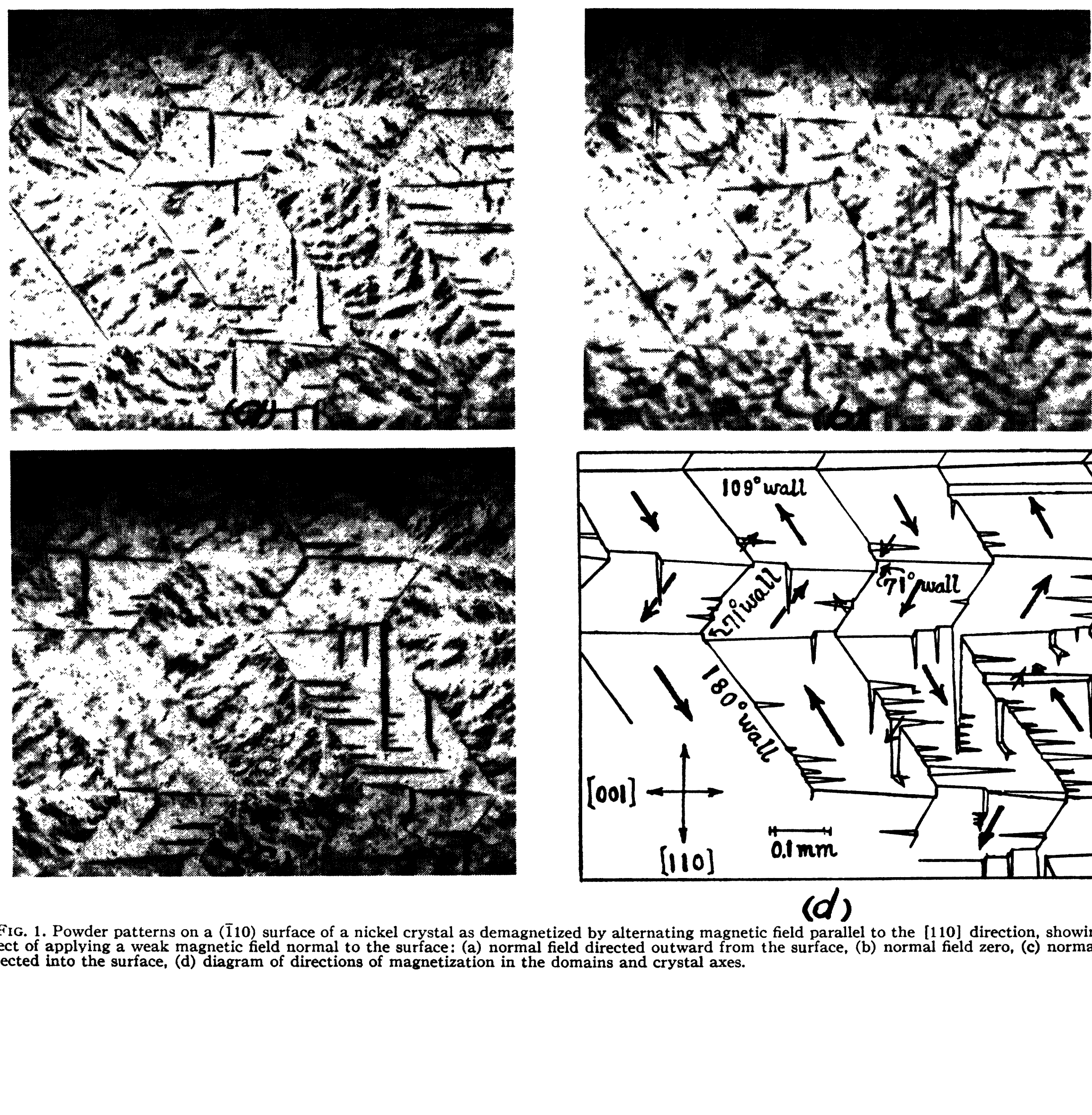

FIG. 1. Powder patterns on a $(\bar{1}10)$ surface of a nickel crystal as demagnetized by alternating magnetic field parallel to the [110] direction, showing the effect of applying a weak magnetic field normal to the surface: (a) normal field directed outward from the surface, (b) normal field zero, (c) normal field directed into the surface, (d) diagram of directions of magnetization in the domains and crystal axes.

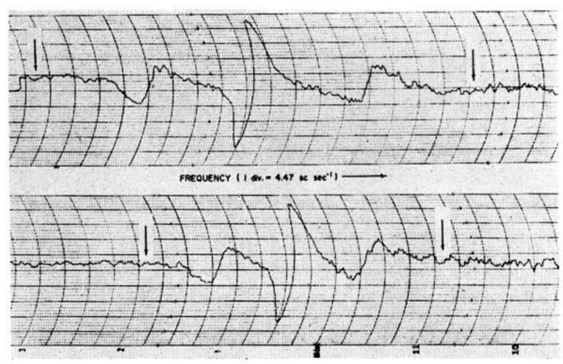

FIG. 1. Absorption curve derivatives of Be^9 magnetic resonances in a single crystal of $BeAl_2O_4$ for two crystal orientations in the magnetic field. The three quadrupole components of each resonance verify that the spin of Be^9 is 3/2. Vertical arrows mark the approximate positions at which additional components should occur if the patterns are quadrupole splittings corresponding to spin 5/2.